Driver Model Based Automated Driving of Long Vehicle Combinations in Emulated Highway Traffic

Peter Nilsson[1], Leo Laine[2], Bengt Jacobson[3] and Niels van Duijkeren[4]

***Abstract*—This paper proposes a framework for automated highway driving of an A-double long vehicle combination. The included driving manoeuvres are maintain lane, lane change to right and left lane, abort lane change to right and left lane, and emergency brake. A combined longitudinal and lateral driver model is used for the generation of longitudinal acceleration and steering requests. The behaviour of the driver model, both regarding heuristics and safety thresholds, is inspired by human cognition and optical flow theory. Traffic situation predictions of feasible lane changes are calculated using the driver model in combination with prediction models of the subject and surrounding vehicles. The traffic situation predictions are used for the evaluation of constraints related to vehicle dynamics, road boundaries and distance to surrounding objects. When the framework is started, the subject vehicle is initiated in the maintain lane state respecting the road speed limit and the distance to surrounding objects. A lane change manoeuvre is performed on request from the driver when the corresponding traffic situation prediction and control request become feasible. The framework has been implemented in simulation environment including a high-fidelity vehicle plant model and models of surrounding vehicles. Simulations show that the framework gives anticipated results when initial conditions are varied. Results are shown for maintain lane and lane change manoeuvres at constant longitudinal velocity, varying from 20-80 km/h and lane changes combined with retardation including leading vehicle braking from different initial velocities ranging from 30-80 km/h.**

I. INTRODUCTION

Long vehicle combinations (LVCs) which are based on the so-called modular concept [1] have shown improved transport productivity compared to existing standard European vehicle combinations. Due to this fact, investigations into an introduction of LVCs are currently ongoing in Sweden [2]. However, by using LVCs the lateral vehicle dynamics in high speed manoeuvres such as lane changes, can be further amplified compared to current vehicle combinations. Typical performance characteristics are rearward amplification (RA) of the lateral acceleration between the first and last vehicle units and lateral off-tracking (LOT) between the first and last axles in the vehicle combination [3]. The amplification of the lateral vehicle dynamics is illustrated in Figure 1, where a lane change manoeuvre at 80 km/h is performed using two different steering wheel frequencies. During the lane change manoeuvre with critical steering wheel frequency input, the RA is approximately 2 and the maximum LOT approximately 1 m. A professional driver of LVCs will take into account the vehicle dynamics and if possible avoid critical steering input frequencies.

An investigation of existing European heavy truck accidents shows that human error is involved in as many as 90 percent of all accidents [4]. When the truck contributes to the accident, the most common cause is limited visibility due to blind spots. A typical blind spot accident is a lane change to right in right-hand traffic. A promising approach to improve the road traffic safety in this traffic situation is the utilization of so-called lane change decision aid systems [5]. In commercially available cars and trucks, the information to the driver from these systems varies from a gentle warning, often optical, to interventions with guiding steering wheel torque. The systems support the driver in deciding whether a lane change is possible or not. The lane change itself must be performed independently by the driver. A foreseen further development of the current lane change assist systems is believed to include fully automated lane change functionality which can improve the traffic safety even further. Currently no such system is available on the market but has been shown in demonstration cars [6].

When comparing a passenger car driver with a LVC driver, it is hypothesized that the latter needs to have higher tactical awareness due to the complexity of handling the LVC in traffic. One reason is that the units in the combination will follow the road curvature while driving in a lane which may cause limited visibility. Another reason is that more nearby vehicles need to be accounted for when driving the LVC. A third reason is that the driver has to account for the amplified vehicle dynamics when negotiating curves and nearby vehicles in the adjacent lanes. If a combined automation of the steering, propulsion, and braking of LVCs is introduced it is also hypothesized that the higher tactical awareness of a manual LVC driver is implemented in the automated system.

One component of the expected higher tactical awareness can be assigned to the handling of the amplified vehicle dynamics and the motion of the surrounding vehicles. Typically, this means that predictions of the vehicle motion and traffic situation are needed for a time horizon of up to 10 s. There are several methods for generating the needed traffic situation predictions (TSPs). Some of these methods are optimization based and use a subject vehicle prediction model in the generation of the TSPs, such as formulating an optimal control problem [7] or by using Rapidly-exploring Random Trees [8]. However, it is not obvious how the objective function should be designed in order to generate a vehicle behaviour with high acceptance from the drivers during manoeuvring. In this paper, it is hypothesised that one feasible way of achieving the tactical

This work is supported by the Swedish national research programme FFI. FFI is financed by Swedish automotive industry and the Swedish research foundation Vinnova.

[1]P. Nilsson and [2]L. Laine are with the Department of Chassis Strategies & Vehicle Analysis, Volvo Group Truck Technology, BF72991, AB4S, SE-405 08, Göteborg, Sweden, peter.q.nilsson@volvo.com, leo.laine@volvo.com

[3]B. Jacobson is with the Vehicle Dynamics group, Division of Vehicle Engineering & Autonomous Systems, Department of Applied Mechanics, Chalmers University of Technology, SE-412 96, Göteborg, Sweden, bengt.jacobson@chalmers.se

[4]N. van Duijkeren is with the Department of Mechanical Engineering, Division PMA, KU Leuven, 3001 Heverlee, Belgium, niels.vanduijkeren@kuleuven.be

awareness of how a LVC driver generates steering, propulsion, and braking can be reached if the actuation request includes a human-like behaviour. Motion actuation requests generated using a driver model inspired by human cognition and optical flow theory, is combined with TSPs for handling the decision making.

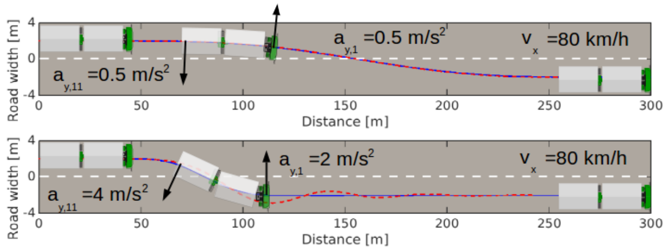

Fig. 1: Illustration of performance characteristics for a LVC in a normal (top) and critical (bottom) highway lane change manoeuvre at 80 km/h with focus on the lateral acceleration rearward amplification and lateral off-tracking. The rearward amplification is approximately 1 in the normal manoeuvre and 2 in the critical manoeuvre. The lateral off-tracking between the first and last axles in the vehicle combination is approximately 0.1 m in the normal manoeuvre and 1 m in the critical manoeuvre.

II. MODELLING

In this section we present the mathematical models used for control design and emulation of the subject and surrounding vehicles.

A. Subject vehicle prediction model

A one-track model is used to describe the truck motion in the traffic situation predictions. The model has been linearised regarding kinematics, steering and tire slip using an assumption of small angles. In order to calculate the position of the truck and its units with respect to the road, a parametrization of the road curvature and heading are included in the model equations. The model differential equations are based on the work in [9] and constitute 16 states and 2 inputs. The equations are given in the Appendix.

B. Driver model

A combined longitudinal and lateral driver model is used for the truck guidance. The control behaviour of the model, both regarding heuristics and safety thresholds, is inspired by human cognition and optical flow theory and follows the approach presented in [10]. This approach is hypothesised to be one feasible way of generating predictions of the traffic situation and actuation requests which holds high acceptance from drivers. The physical parameters of the model are illustrated in Figure 2.

1) Lateral driver model: The driver's steering utilization law is based on a two-point visual model [11] formulated as

$$\dot{\delta}_{\mathrm{des}} = k_{\mathrm{f}} \cdot \dot{\theta}_{\mathrm{f}} + k_{\mathrm{n}} \cdot \dot{\theta}_{\mathrm{n}} + k_{\mathrm{I}} \cdot \theta_{\mathrm{n}} \tag{1}$$

where $\dot{\delta}_{\mathrm{des}}$ is the time derivative of the desired steering wheel angle, θ_{n} is the perceived angle to a near point, and $\dot{\theta}_{\mathrm{f}}$ and $\dot{\theta}_{\mathrm{n}}$ are the angular velocities of the perceived angles to a far and

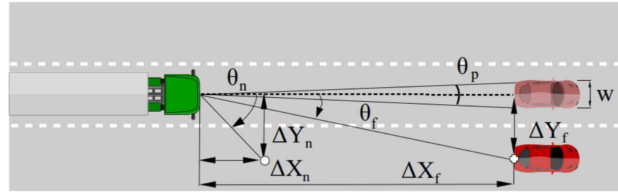

Fig. 2: Illustration of the optical parameters used in the driver model. The parameters are: optical size θ_{p}, angle to a near-point θ_{n}, and a far-point θ_{f}. The distance w is the width of the lead vehicle and ΔX_{n} and ΔX_{f} are the distances to the near and far-points, respectively.

near point, respectively, see Figure 2. The perceived angles and angular velocities are calculated as

$$\theta_{\mathrm{n}} = \arctan\left(\frac{\Delta Y_{\mathrm{n}}}{\Delta X_{\mathrm{n}}}\right) - \phi \tag{2}$$

$$\dot{\theta}_{\mathrm{n}} = \frac{\Delta X_{\mathrm{n}} \cdot \Delta v_{Y_{\mathrm{n}}} - \Delta Y_{\mathrm{n}} \cdot \Delta v_{X_{\mathrm{n}}}}{\Delta Y_{\mathrm{n}}^2 - \Delta X_{\mathrm{n}}^2} - \dot{\phi} \tag{3}$$

$$\dot{\theta}_{\mathrm{f}} = \frac{\Delta X_{\mathrm{f}} \cdot \Delta v_{Y_{\mathrm{f}}} - \Delta Y_{\mathrm{f}} \cdot \Delta v_{X_{\mathrm{f}}}}{\Delta Y_{\mathrm{f}}^2 - \Delta X_{\mathrm{f}}^2} - \dot{\phi} \tag{4}$$

where ΔX_{n}, ΔY_{n}, ΔX_{f}, ΔY_{f}, $\Delta v_{X_{\mathrm{n}}}$, $\Delta v_{Y_{\mathrm{n}}}$, $\Delta v_{X_{\mathrm{f}}}$ and $\Delta v_{Y_{\mathrm{f}}}$ are the relative longitudinal and lateral distances and velocities between the truck and the near and far points respectively, expressed in the global coordinate frame. The parameters ϕ and $\dot{\phi}$ are the yaw angle and the yaw angular velocity of the tractor unit.

2) Longitudinal driver model: The desired braking and propulsion adjustments, based on [12], use a reference acceleration $a_{\mathrm{x,ref}}$ calculated as

$$a_{\mathrm{x,ref}} = (1 + \dot{\tau}_{\mathrm{m}}) \cdot \frac{\Delta v_{\mathrm{x}}^2}{(\Delta X_{\mathrm{f}} - v_{\mathrm{o}} \cdot t_{\mathrm{h}})} \tag{5}$$

$$a_{\mathrm{x,min}} \leq a_{\mathrm{x,ref}} \leq a_{\mathrm{x,max}} \tag{6}$$

where, Δv_{x} is the longitudinal velocity difference between the truck front axle and the lead vehicle, ΔX_f is the far point distance, and t_h is the desired final temporal headway. The constant parameter $\dot{\tau}_{\mathrm{m}}$ is an approximation of the time derivative of time-to-collision. The magnitude of $a_{\mathrm{x,ref}}$ is constrained by the minimum $a_{\mathrm{x,min}}$ and maximum accelerations $a_{\mathrm{x,max}}$. In addition, initially during braking and propulsion, the retardation and acceleration are ramped up to their requested values using a limit on the jerk.

The initiation of braking and propulsion are based on margin values of the optical expansion rate $\dot{\theta}_{\mathrm{p,m}}$ and the temporal headway $t_{\mathrm{h,m}}$

$$\dot{\theta}_{\mathrm{p,m}} \leq \dot{\theta}_p \leq -\dot{\theta}_{\mathrm{p,m}},\ t_{\mathrm{h,m}} + \varepsilon_{\mathrm{t}} \leq t_{\mathrm{h}} \leq t_{\mathrm{h,m}} \tag{7}$$

where ε_{t} is a small constant parameter. The optical expansion rate $\dot{\theta}_{\mathrm{p}}$ and the temporal headway t_{h} are calculated as

$$\dot{\theta}_p = \frac{-4 \cdot w \cdot \Delta v_{\mathrm{x}}}{w^2 + 4 \cdot \Delta X_{\mathrm{f}}^2} \tag{8}$$

$$t_{\mathrm{h}} = \frac{\Delta X_{\mathrm{f}}}{v_{\mathrm{x,1}}} \tag{9}$$

where w is the width of the lead vehicle and $v_{\mathrm{x,1}}$ is the longitudinal velocity of the truck front axle.

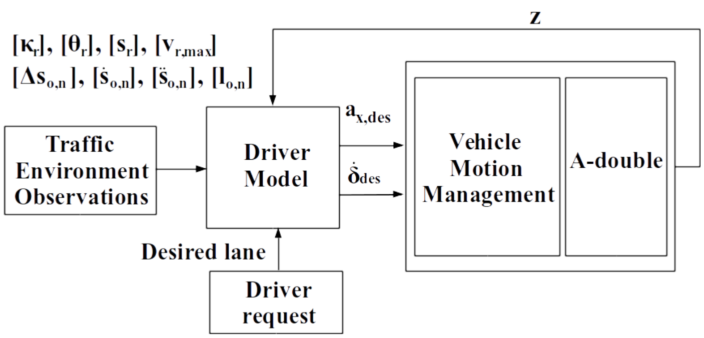

Fig. 3: Control design of automated driving. The inputs to the driver model are: state measurements z and traffic situation observations including; road curvature $[\kappa_\mathrm{r}]$, road heading angle $[\theta_\mathrm{r}]$, road distance $[s_\mathrm{r}]$ and max road velocity $[v_\mathrm{r,max}]$. Also, the relative distance $[\Delta s_\mathrm{o,n}]$, velocity $[\dot{s}_\mathrm{o,n}]$, acceleration $[\ddot{s}_\mathrm{o,n}]$ and lane $[l_\mathrm{o,n}]$ of surrounding vehicles. The outputs from the driver model are the desired longitudinal acceleration $a_\mathrm{x,des}$ and the desired road wheel steering angle rate $\dot{\delta}_\mathrm{des}$.

C. Subject vehicle plant model

A Volvo in-house developed high fidelity two-track model library is used emulate the truck plant model dynamics. The model includes detailed sub-models of the vehicle chassis, cab suspensions, steering system, powertrain, and brakes. The frame torsion flexibility of the tractor and semi-trailers is considered by using multiple frame bodies connected through springs. The Magic Formula tire model [13] with combined slip, dynamic relaxation, and rolling resistance, is used for all tires in the vehicle combination.

D. Surrounding vehicle prediction and plant model

The dynamics of the surrounding vehicles are modelled as individual point-masses including a predetermined acceleration profile. The motion is described using the following set of differential equations

$$\frac{d}{dt}\begin{bmatrix} s_\mathrm{o,n} \\ \dot{s}_\mathrm{o,n} \end{bmatrix} = \begin{bmatrix} 0 & 1 \\ 0 & 0 \end{bmatrix} \cdot \begin{bmatrix} s_\mathrm{o,n} \\ \dot{s}_\mathrm{o,n} \end{bmatrix} + \begin{bmatrix} 0 \\ 1 \end{bmatrix} \cdot \ddot{s}_\mathrm{o,n} \tag{10}$$
$$n = 1,\ldots,6 \text{ are the number of surrounding vehicles}$$

where $s_\mathrm{o,n}, \dot{s}_\mathrm{o,n}$ and $\ddot{s}_\mathrm{o,n}$ are the position, velocity and acceleration tangential to the defined road geometry. Besides the defined states (10), the vehicles also include information of its length and width dimensions and current lane identity. When the model is used in predictions of the traffic situation a constant velocity is assumed during the entire prediction horizon.

III. CONTROL DESIGN

In this section the control design for automated driving in highway traffic with multiple lanes on a one way road is presented. The first section introduces the closed loop system of the driver model and the A-double and motion management models. The second section introduces the basis of the closed loop simulations used for predicting the traffic situation.

A. Closed loop system

1) Longitudinal control: The longitudinal control part of the driver model is formulated in (5)-(9). The longitudinal control design is formulated as an iteratively updated feedforward controller requesting a reference acceleration $a_\mathrm{x,ref}$ to maintain constant $\dot{\tau}_\mathrm{m}$. The margin values in (7) are used for switching between no action, propulsion and braking.

2) Lateral control: The lateral control part of the driver model is formulated in (1). In order to increase the insight of the lateral control, one approach is to reformulate the perceived angle and the perceived angular velocities into the perpendicular distance of the first truck axle projected on the lane geometry, e_1. The time derivative of e_1 can be expressed as

$$\dot{e}_1 = v_\mathrm{x,1} \cdot sin(\phi) + \left(v_\mathrm{y,1} + 1.5 \cdot \dot{\phi}\right) \cdot cos(\phi) \tag{11}$$

where $v_\mathrm{x,1}$ and $v_\mathrm{y,1}$ are the longitudinal and lateral velocities of the first tractor axle and $\dot{\phi}$ and ϕ are the yaw angle velocity and the yaw angle of the tractor unit expressed in a road coordinate system.
Further, we assume small angles, zero road curvature and that the second part of (11) can be ignored. By formulating (1) using the Laplace variable s and combining with (2) and (11), the lateral control can be formulated as

$$\delta_\mathrm{des} = \left(\left(\frac{k_\mathrm{n}}{\Delta X_\mathrm{n}} + \frac{k_\mathrm{f}}{\Delta X_\mathrm{f}} + \frac{k_\mathrm{I}}{v_\mathrm{x,1}} \right) + \frac{k_\mathrm{I}}{\Delta X_\mathrm{n}} \cdot \frac{1}{s} + \left(\frac{k_\mathrm{n} + k_\mathrm{f}}{v_\mathrm{x,1}} \right) \cdot s \right) \cdot e_1 \tag{12}$$

With the above assumptions, the lateral control is expressed as a PID controller of e_1 where $v_\mathrm{x,1}$ and ΔX_f are used for gain scheduling.

B. Closed loop predictions

Predictions of the traffic situation are performed in a receding horizon fashion as closed loop simulations (CLSs) including the driver model and prediction models of the subject and the surrounding vehicles. The numerical simulations are carried out using the forward Euler method with step size t_e and with prediction time t_p. Starting from the subject vehicle lane, we identify the closest lanes to the left and right. For each existing lane we identify the first leading and trailing vehicle within the distance horizon s_f. If no vehicle exists within s_f, a dummy vehicle is added at s_f, and given the maximum road velocity $v_\mathrm{r,max}$. The distances and velocities of the surrounding vehicles are used in the generation of optical parameters for the driver model. The closed loop simulations are initiated by defining the initial prediction model states to measured state values. For each step in the simulations, the CLSs are evaluated regarding constraints related to vehicle dynamics,

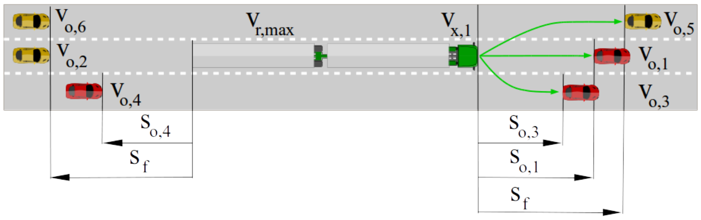

Fig. 4: Closed loop simulations and actuation requests are calculated for the current and adjacent lanes. For each identified lane, the first vehicle ahead and behind the truck within the distance s_f are identified (red). If no vehicles exists within s_f, a dummy vehicle (yellow) is defined at s_f, and given the road speed limit velocity.

lane boundaries and surrounding vehicles according to

$$v_{\mathrm{x,min}} \leq v_{\mathrm{x,1}} \leq v_{\mathrm{r,max}} \tag{13}$$

$$-a_{\mathrm{y,max}} \leq a_{\mathrm{y,i}} \leq a_{\mathrm{y,max}} \tag{14}$$

$$s_{\mathrm{o,j,leading}} \geq s_1 \tag{15}$$

$$s_{\mathrm{o,j,trailing}} \leq s_{11} \tag{16}$$

$$e_{\mathrm{j,k,min}} \leq e_{\mathrm{i}} \leq e_{\mathrm{j,k,max,}} \tag{17}$$

$i = 1, 11$ are the numbers of the axles in the vehicle combination

$j = 0, 1, 2$ are the number of the CLSs

$k = 1, ..., 11$ are number of the current driving state

where $v_{\mathrm{x,min}}$ is the lower limit of the longitudinal velocity and $v_{\mathrm{x,1}}$ is the longitudinal velocity of the first truck axle. Furthermore, $a_{\mathrm{y,max}}$ is the maximum allowed lateral acceleration, $a_{\mathrm{y,1}}$ and $a_{\mathrm{y,11}}$ are the lateral accelerations of the first and the last truck axles. The distances $e_{\mathrm{j,k,min}}$ and $e_{\mathrm{j,k,max}}$ are the minimum and maximum allowed perpendicular distances from the lane center line, $s_{\mathrm{o,j,leading}}$ and $s_{\mathrm{o,j,trailing}}$ are the distances to the leading and trailing vehicles, s_1, s_{11}, e_1 and e_{11} are the distances and the perpendicular distances of the first and the last truck axle projected on the lane geometry. The upper and lower values of the constraints related to the lane boundaries are dependent on the current driving state. If any constraint is violated, the CLS is identified as infeasible, which is used in the decision making. In Figure 4, the parameters used in the CLS generation are illustrated.

IV. FUNCTION REFERENCE ARCHITECTURE

The vehicle's motion functionality was partitioned and developed with regards to a function reference architecture which is used within Volvo GTT. The partitioning was done into a hierarchical structure to separate motion functionality in long term, mid term, and short term planning, execution, and tracking. This, because it is foreseen that different spatial and time horizon predictions and planning will be conducted which requires modelling with different granularity of the subject vehicle and the surrounding environment for efficient computations in the intended time and spatial horizon [14]. In addition, the reference architecture also addresses that internal quality attributes such as adaptability, changeability, and stability are achieved [15]. The external quality attributes of the architecture such as interoperability and functional behaviour need to be evaluated by simulations and physical testing [15]. In this section the functionality domains (FDs) Vehicle motion management (VMM) and Traffic situation management (TSM) are described. The VMM has a time horizon of up to 1 s and has a reactive and coordinative character with vehicle stability as a core functionality. The TSM has a time horizon of up to 10 s and the prediction has a tactical character. The functionality domains of strategical character, with a time horizon larger than 10 s, are omitted.

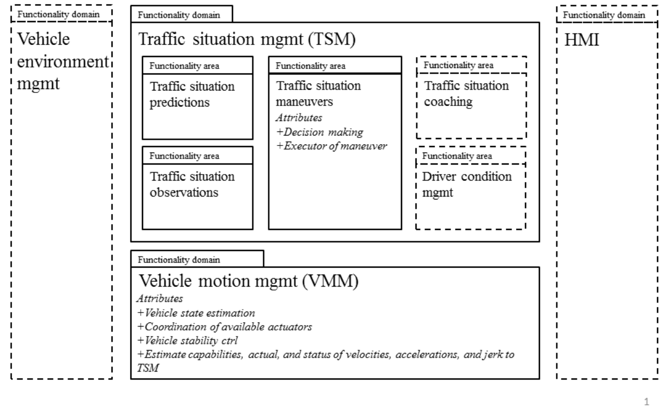

Fig. 5: Function reference architecture: solid boxes are explained, dashed boxes are only for orientation.

A. *Vehicle motion management (VMM)*

The VMM FD encapsulates the knowledge of specific available actuation topology within the vehicle combination. The main attributes are vehicle state estimation, transforming acceleration or speed requests into available actuation requests. In this framework, control allocation has been used for coordinating propulsion, braking, and steering [16]. The control allocation weighting for, e.g. braking in-between axles, has been adapted to commercial heavy vehicles [17]. The control allocation formulation has also been adapted for large articulation angles between the vehicle units and wheel steer angles by deriving the actuation control efficiency matrix $B(\theta_i, \delta_j)$ by using Lagrange formulation [18]. This latter was not included in this study due to that small articulation angles and a steered axle were only available on the first vehicle unit's front axle. Another attribute is to provide vehicle actuation capabilities, status, and actual values of the vehicle states to the TSM FD.

B. *Traffic situation management (TSM)*

In the functionality domain TSM there are three main functionality areas (FAs) which will be explained in this section; Traffic situation observation, Traffic situation predictions, and Traffic situation manoeuvres.

1) Traffic situation observation: The scope of this functionality domain is to include the current estimated subject vehicle road positioning and states, surrounding vehicle position and their current vehicle states, number of lanes, and road information ahead. In simulations, spatial observation included surrounding vehicles and road information ahead and behind up to ± 175 m.

2) Traffic situation prediction (TSP): In this framework, a maximum of three CLSs, see Section III-B are performed and evaluated at each actuation request update instant. The simulated CLSs, illustrated in Figure 5, are associated with the truck lane and the closest adjacent lanes. Time traces for the actuation request (desired steering angle and longitudinal acceleration) for each CLS are calculated in TSP.

3) Traffic situation manoeuvres: The main attribute of FA traffic situation manoeuvres is the decision making. The decision making process is implemented as a finite state-machine utilizing the driving states. The finite state-machine including the switching conditions is illustrated in Figure 7. Here, $t_{\mathrm{h,o}}$ is the temporal headway to the vehicles in front and behind the truck, $t_{\mathrm{lc,m}}$ is the used margin value for lane change initialisation, e_1, e_{11} are the perpendicular distances of the first and the last truck axles projected on the lane center line, d is the lane width, ε is a constant parameter and e_{m} is the used margin value for lane change completion. If the vehicle is in the emergency brake state, the state-machine will try return to the previous state during 50 iterations. The illustration of this part is omitted in Figure 7. In this framework, seven driving manoeuvres are defined: maintain lane, lane change to right and left lane, abort lane change to right and left lane and emergency brake. The emergency brake manoeuvre is always characterized by the actuation request: maximum retardation $a_{\mathrm{x,min}}$ and zero road wheel steering angle. Apart from the maintain lane and emergency brake manoeuvres, which only require actuation request connected to one TSP, actuation requests connected to two TSPs are always combined to define one complete manoeuvre. The reason for this is the approach used for defining the manoeuvres and the subject vehicle road lane identity. The subject vehicle lane identification is based on the position of the front axle. For a lane change to right manoeuvre, this means that the initially used actuation request is coupled to the TSP defined for the lane to the right of the truck lane (TSP 1). When the vehicle has shifted from the initial lane to the target lane, the used actuation request is instead coupled to the TSP defined for the current truck lane (TSP 0). In Figure 6 the connection between the actuation request and the TSPs in a lane change to right lane manoeuvre is illustrated for the initial part of the manoeuvre (top) and the final part of the manoeuvre (bottom).

In order to handle the combinatorics of actuation requests which are required to carry out the different manoeuvres, 12 driving states are defined. The used driving states are: maintain lane, lane change to right requested, lane change to left requested, lane change to right initial, lane change to right final, lane change to left initial, lane change to left final, abort lane change to right initial, abort lane change to right final, abort lane change to left initial, abort lane change to left final and emergency brake. In Table I, the coupling between the driving manoeuvres, driving states and the actuation request numbers are given.

V. SIMULATION RESULTS

In this section simulation results from two lane change scenarios are presented. Both scenarios are realized using a straight three lane one way road with two surrounding vehicles in each lane. A straight road is selected for clarity when presenting the results. Simulations on a realistic curvy road show similar results but have been omitted. The parameters used in the scenarios are given in Table II. In the first scenario, lane changes to the right are carried out at varying constant vehicle velocities in the range of 20-80 km/h. The absolute magnitude of the headway to all surrounding vehicles are equal and are specified slightly larger than the threshold value for lane change initialisation. The headway is kept constant during the entire simulation. The initial conditions of the scenario are illustrated in Figure 8 (top). In the second scenario, lane changes to the right combined with braking are studied. The initial truck velocities are chosen in the range of 30-80 km/h. The magnitudes of the headway to the surrounding vehicles as well as the threshold values for lane change initialisation are varied in the range of 0.5-2.0 s. In the second scenario, the initial conditions regarding the surrounding vehicles are the same as in the first scenario. However, when the first axle of the truck enters the target lane the leading vehicle starts braking, illustrated in Figure 8 (bottom). At this point, the truck will either fulfil the initiated lane change, return to the initial lane using the abort manoeuvre or enter the emergency brake manoeuvre.

The simulations are carried out in Matlab/Simulink. The high-fidelity vehicle model, the road description and the motion of the surrounding vehicles are modelled in Simulink. The controller, which is written in C++, is interfaced using a Matlab S-function.

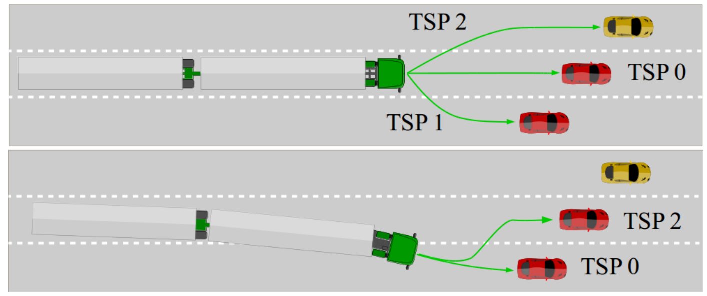

Fig. 6: Illustration of the actuation requests and the corresponding TSP in a lane change to right lane manoeuvre. In the first part of the manoeuvre, the actuation request connected to the TSP defined for the lane to the right of the truck lane (TSP 1) is used for control (top). When the vehicle has shifted to the target lane, the actuation request connected to the current lane (TSP 0) is used for control (bottom).

TABLE I: Relation between the driving manoeuvres, driving states and actuation request number/TSP number.

Driving manoeuvres	Driving states	Actuation request No. Current	Right	Left
Maintain lane	Maintain lane (0)	0		
	Lane change to right requested (-1)	0		
	Lane change to left requested (1)	0		
Lane change to right lane	Lane change to right initial (-2)		1	
	Lane change to right final (-3)	0		
Lane change to left lane	Lane change to left initial (2)			2
	Lane change to left final (3)	0		
Abort lane change to right lane	Abort lane change to right initial (-4)			2
	Abort lane change to right final (-5)	0		
Abort lane change to left lane	Abort lane change to left initial (4)		1	
	Abort lane change to left final (6)	0		

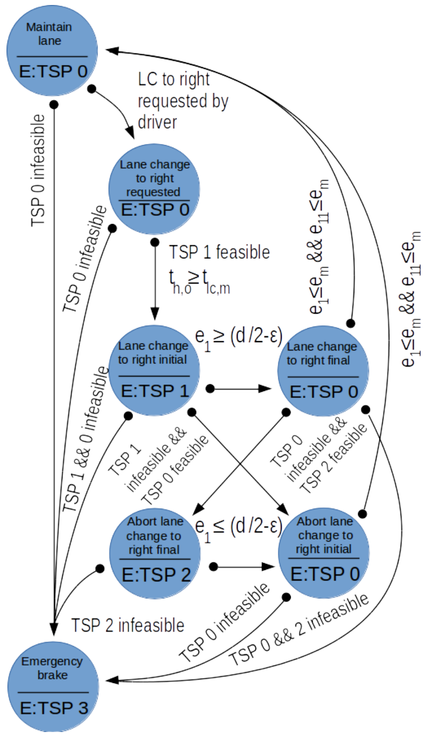

Fig. 7: Finite state machine for decision making. Only right side manoeuvres illustrated. Manoeuvres to the left side are mirrored.

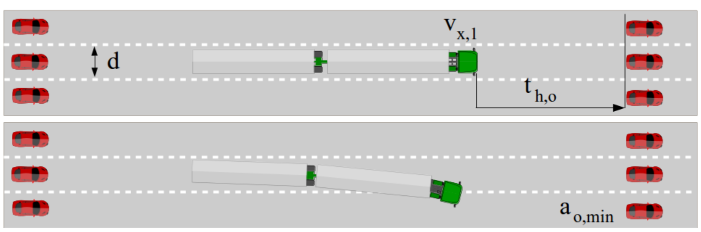

Fig. 8: The top panel illustrates the initial conditions for both simulated lane change scenarios. The bottom panel shows the condition for when the leading vehicle in the target lane decelerates, used in Scenario II.

A. Scenario I: Lane change at constant speed

In this section we evaluate the performance of the framework for lane changes at constant velocities in the range of 20-80 km/h. Important characteristics of a lane change at a constant velocity of 80 km/h are shown in Figure 9. At time 5 s, a lane change to right is requested and initiated and the driving state is shifted from maintain lane (0) to lane change to right requested (-1) to lane change to right initial (-2). At time 8 s, the front axle of the truck enters the target lane and the driving state is changed to lane change to right final (-3). The lane change is completed at the time 17 s, occurring when the 1st and 11th axles of the truck are within the distance e_m from the target lane center line. The driving state is then changed back to maintain lane (0). The maximum absolute value of the steering wheel amplitude during the manoeuvre is approximately 13 ° and the maximum absolute lateral accelerations of the 1st and 11th truck axle are 0.8 m/s^2 and 1 m/s^2 respectively. the latter results in a rearward amplification of approximately 1.5.

TABLE II: Parameters used in the simulated scenarios.

Scenario I parameters	Symbol	Value	Unit
Truck velocity	$v_{x,1}$	20:5:80	km/h
Temporal headway to surr. vehicles	$t_{h,o}$	2.2	s
Margin value for lane change initiation	$t_{lc,m}$	2.0	s
Desired final temporal headway	$t_{h,f}$	2.0	s
Scenario II parameters			
Initial truck velocity	$v_{x,1,init}$	30:10:80	km/h
Final truck velocity	$v_{x,1,final}$	20:10:70	km/h
First axle offset for start of vehicle ret.	$e_{1,start}$	-2.0	m
Initial temporal headway to surr. vehicles	$t_{h,o}$	0.7:0.5:2.2	s
Lead vehicle deceleration	$a_{o,min}$	-6.9	m/s^2
Margin value for lane change initiation	$t_{lc,m}$	0.5:0.5:2.0	s
Desired final temporal headway	$t_{h,f}$	0.5:0.5:2.0	s
Traffic situation prediction parameters			
Step size	t_e	0.05	s
Prediction time	t_p	3.75	s
Maximum distance to surr. vehicles	s_f	100	m
Maximum truck retardation	$a_{x,min}$	-5.9	m/s^2
Maximum truck acceleration	$a_{x,max}$	0.3	m/s^2
Lateral acceleration limit	$a_{y,max}$	3.0	m/s^2
Tau rate	$\dot{\tau}_{s,m}$	-0.425	-
Optical expansion rate margin value	$\dot{\theta}_{p,m}$	0.2	°/s
Time gap margin value	$t_{s,m}$	2.5	s
Gain perceived angle rate, far point	k_f	3.07	-
Gain perceived angle rate, near point	k_n	1.48	-
Gain perceived angle, near point	k_I	0.41	-
Near point distance	x_n	5	m
Lane width	d	4	m
Decision making parameters			
Distance offset for lane change completion	e_m	0.3	m

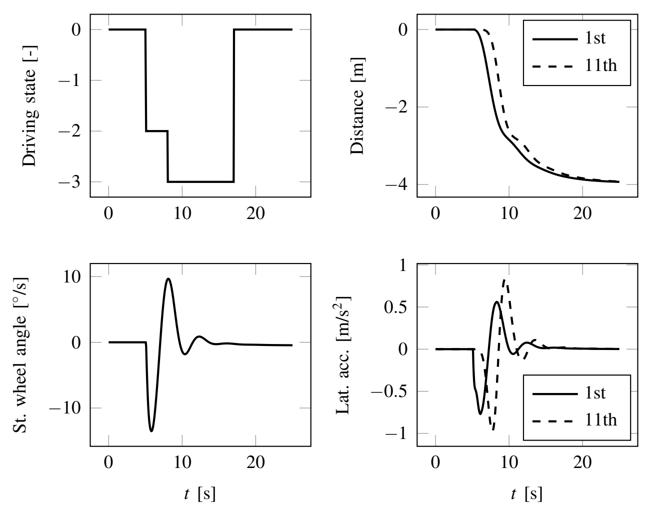

Fig. 9: Important characteristics of a lane change at the constant velocity of 80 km/h: driving state (top left), lane center distance offset (top right), steering wheel angle (bottom left), and lateral acceleration (bottom right).

In Figure 10, the main characteristics of lane changes at constant velocities within the range of 20-80 km/h are shown. The lane change durations and the maximum absolute steering wheel angles vary between 12-18 s and 13-23 °, respectively. The maximum absolute lateral accelerations of the 1st and 11th truck axle vary between 0.2-0.8 m/s^2 and 0.1-1 m/s^2, respectively. The resulting rearward amplifications range between 0.8-1.5.

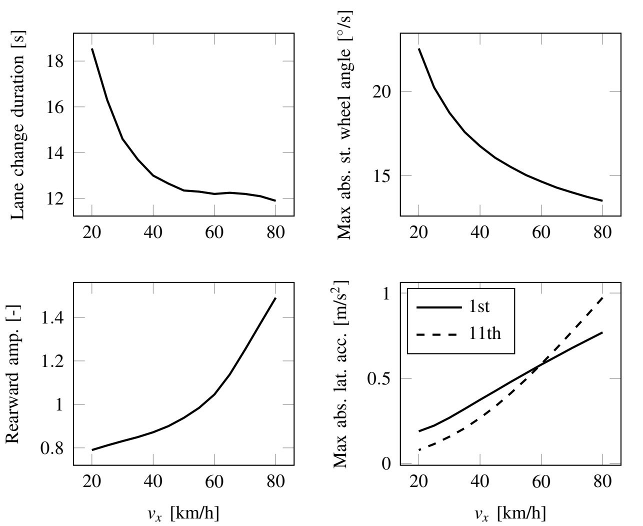

Fig. 10: The main characteristics of lane changes at constant velocities in the range of 20-80 km/h: lane change duration (top left), maximum absolute steering wheel angle amplitude (top right), rearward amplification (bottom left), and maximum absolute lateral acceleration amplitude (bottom right).

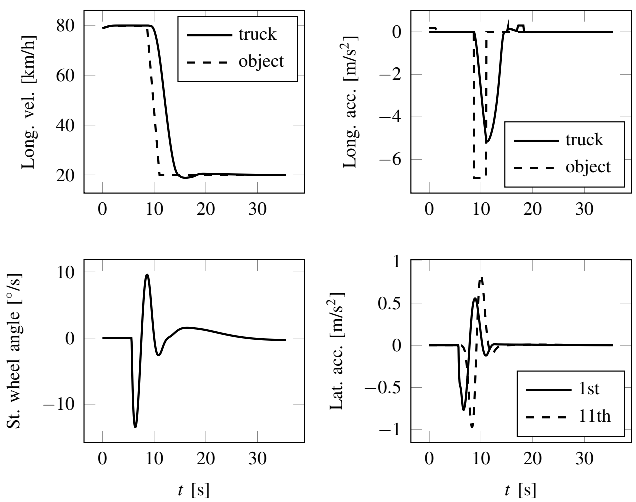

Fig. 11: Important characteristics of a lane change combined with braking where the initial and final velocities are 80 km/h and 20 km/h, respectively: longitudinal velocity (top left), longitudinal acceleration (top right), steering wheel angle (bottom left), and lateral acceleration (bottom right). The absolute magnitude of the initial headway to all vehicles is 2.2 s and the margin value for lane change initialisation is 2.0 s.

B. Scenario II: Lane change combined with braking

In this section we evaluate the performance of the framework regarding lane changes combined with braking. Firstly, the initial and final truck velocities are varied in the range of 30-80 km/h and 20-70 km/h, respectively. Secondly, the margin value for lane change initialisation is varied in the range of 0.5-2.0 s. In Figure 11, important characteristics of one lane change combined with braking are presented. In this example, the initial and final truck velocities are 80 and 20 km/h, respectively. The absolute magnitude of the initial headway to all vehicles is 2.2 s and the margin value for lane change initiation is 2.0 s. At time 5 s, the truck velocity is 80 km/h and a lane change to right is initiated. At time 7.3 s, the truck front axle enters the target lane and the leading vehicle brakes from 80 to 20 km/h using a retardation of 6.9 m/s^2. During the truck braking, the maximum retardation of the truck reaches 5.1 m/s^2 and the headway to the lead vehicle reduces to a minimum of 1.3 s. The maximum absolute value of the steering wheel amplitude during the manoeuvre is approximately 13 ° and the maximum absolute lateral accelerations of the 1st and 11th truck axles are approximately 0.6 m/s^2 and 0.8 m/s^2, respectively. The latter results in a rearward amplification of approximately 1.3.

In Figure 12, the margin value for lane change initialisation is varied in the range of 0.5-2.0 s. For margin values lower than 1.5 s the framework is not longer able to finalize all initiated lane changes but enters the abort or emergency brake manoeuvres.

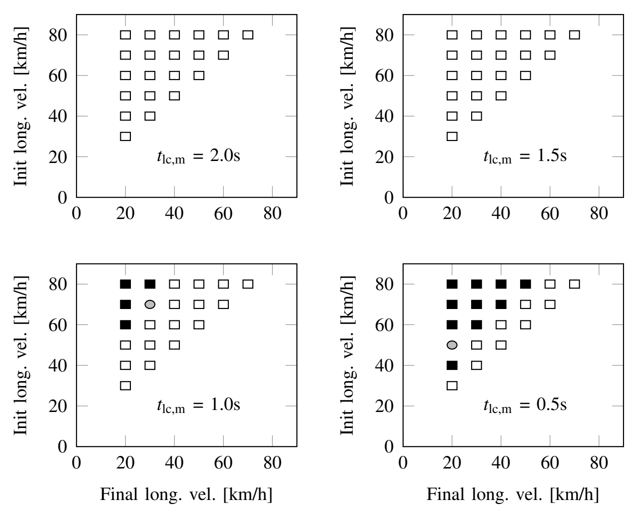

Fig. 12: Performance of the framework for lane changes combined with braking where the initial and final truck velocities are varied in the range of 30-80 km/h and 20-70 km/h, respectively. The unfilled rectangles represents a successfully completed lane change manoeuvre, filled circles represents a successfully completed abort manoeuvre and the filled rectangles represents an emergency brake manoeuvre. The margin values for lane change initialisation are 2.0 s (top left), 1.5 s (top right), 1.0 s (bottom left) and 0.5 s (bottom right).

VI. CONCLUSIONS

This paper presents a driver model based framework for automated highway driving of an A-double LVC. The included driving manoeuvres are maintain lane, lane change to right and left lane, abort lane change to right and left lane, and emergency brake. The framework has been implemented in a simulation environment including a high-fidelity vehicle plant model and surrounding vehicles. Simulations of two lane-change scenarios have been run on a straight three lane one way road including multiple surrounding vehicles. The results shows that the framework is able to perform lane keeping and lane change manoeuvres at constant and varying longitudinal velocities in the range of 20-80 km/h. Furthermore, the results shows that the framework can accomplish an abort manoeuvre back to the initial lane or an emergency brake manoeuvre, if the feasibility of the initiated lane change manoeuvre is not fulfilled.

However, it is pointed out that the complexity of environmental perception and vehicle state estimation have not been included in the work. In addition, the TSPs are based on a driver model in which the parameters have been defined using on-road measurements in smooth driving. The ability to generate trajectories for critical manoeuvres might therefore be limited; adding several selectable sets of driver model parameters would make it possible to find feasible solutions.

APPENDIX

In the traffic situations prediction the following differential equations are used to describe the truck motion in the lane:

$$
\begin{aligned}
&\dot{z}_1 = 47.0\cdot\delta - z_{10}\cdot z_3 + 1.9\cdot z_4 + 0.9\cdot z_6 - 0.002\cdot z_8 \\
&\quad + (-70.7\cdot z_1 + 9.7\cdot z_3 + 21.7\cdot z_5 + 4.5\cdot z_7 - 0.02\cdot z_9)/z_{10} \\
&\dot{z}_2 = z_3 - \kappa_{R,1}\cdot(z_{10}\cdot\cos(z_2) - (z_1 + z_3\cdot 1.5)\cdot\sin(z_2)) \\
&\dot{z}_3 = 25.0\cdot\delta - 1.9\cdot z_4 - 0.8\cdot z_6 + 0.002\cdot z_8 + (27.6\cdot z_1 \\
&\quad -174.2\cdot z_3 - 20.8\cdot z_5 - 4.3\cdot z_7 + 0.02\cdot z_9)/z_{10} \\
&\dot{z}_4 = z_5 \\
&\dot{z}_5 = -25.5\cdot\delta - 4.0\cdot z_4 + 2.5\cdot z_6 - 0.007\cdot z_8 + (-36.5\cdot z_1 \\
&\quad +165.4\cdot z_3 - 10.9\cdot z_5 + 13.0\cdot z_7 - 0.05\cdot z_9)/z_{10} \\
&\dot{z}_6 = z_7 \\
&\dot{z}_7 = 0.6\cdot\delta + 2.3\cdot z_4 - 22.9\cdot z_6 - 0.9\cdot z_8 + (19.9\cdot z_1 \\
&\quad -216.8\cdot z_3 - 169.7\cdot z_5 - 125.8\cdot z_7 - 7.2\cdot z_9)/z_{10} \\
&\dot{z}_8 = z_{10} \\
&\dot{z}_9 = -0.19\cdot\delta + 5.1\cdot z_4 + 22.7\cdot z_6 - 7.1\cdot z_8 + (-12.5\cdot z_1 \\
&\quad -+195.8\cdot z_3 + 168.6\cdot z_5 + 68.2\cdot z_7 - 54.7\cdot z_9)/z_{10} \\
&\dot{z}_{10} = a_{x,1} \\
&\dot{z}_{11} = (a_{x,1,\mathrm{des}} - a_{x,1})/\tau \\
&\dot{z}_{12} = 1/(1-\kappa_{R,1}\cdot z_{13})\cdot(z_{10}\cdot\cos(z_2) - (z_1 + z_3\cdot 1.5)\cdot\sin(z_2)) \\
&\dot{z}_{13} = z_{10}\cdot\sin(z_2) + (z_1 + z_3\cdot 1.5)\cdot\cos(z_2) \\
&\dot{z}_{14} = 1/(1-\kappa_{R,4}\cdot z_{15})\cdot((-24.6\cdot z_3 - 22.7\cdot z_5 - 12.3\cdot z_7 - 7.7\cdot z_9 \\
&\quad -z_4\cdot z_{10} - z_6\cdot z_{10} - z_8\cdot z_{10} + z_1)\cdot -\sin(z_2 + z_4 + z_6 + z_8 \\
&\quad -\theta_{R,4} + \theta_{R,1}) + z_{10}\cdot\cos(z_2 + z_4 + z_6 + z_8 - \theta_{R,4} + \theta_{R,1})) \\
&\dot{z}_{15} = ((-24.6\cdot z_3 - 22.7\cdot z_5 - 12.3\cdot z_7 - 7.7\cdot z_9 - z_4\cdot z_{10} - z_6\cdot z_{10} \\
&\quad -z_8\cdot z_{10} + z_1)\cdot\cos(z_2 + z_4 + z_6 + z_8\theta_{R,4} + \theta_{R,1}) + z_{10}\cdot\sin(z_2 + z_4 \\
&\quad +z_6 + z_8 - \theta_{R,4} + \theta_{R,1})) \\
&\dot{z}_{16} = \dot{\delta} \\
&\quad z = \left[\dot{y}_1, \phi, \dot{\phi}, \theta_1, \dot{\theta}_1, \theta_2, \dot{\theta}_2, \theta_3, \dot{\theta}_3, v_{x,1}, a_{x,1}, s_1, e_1, s_{11}, e_{11}, \dot{\delta}\right] \\
&\quad u = [a_{x,1,\mathrm{des}}, \delta]
\end{aligned}
$$

The states $\dot{y}_1$, ϕ and $\dot{\phi}$ are the lateral velocity, yaw angle and yaw rate of the first vehicle axle, $\theta_1, \theta_2, \theta_3, \dot{\theta}_1, \dot{\theta}_2$ and $\dot{\theta}_3$ are the articulation angles and the rate of the articulation angles of the towed units. $v_{x,1}$ and $a_{x,1}$ are the longitudinal velocity and acceleration of the first vehicle axle. s_1, s_{11}, e_1 and e_{11} are the distances and the perpendicular distances of the first and the last vehicle axles projected on the lane geometry. The variables $\kappa_{R,1}, \kappa_{R,4}, \theta_{R,1}, \theta_{R,4}$ are the road curvature and the road heading angles of the first and last vehicle axles. The parameter τ is a time constant for the longitudinal dynamics. The model inputs are the longitudinal acceleration of the first vehicle axle $a_{x,1,\mathrm{des}}$ and the road wheel steering angle δ. All units are SI.

REFERENCES

[1] J. Aurell and T. Wadman, "Vehicle combinations based on the modular concept," NVF-reports, Report 1/2007, Tech. Rep., 2007.

[2] http://www.vinnova.se/sv/Resultat/Projekt/Effekta/DUO2---Energieffektiva-fordonskombinationer/, 2014.05.23.

[3] M. S. Kati, "Definitions of performance based characteristics for long heavy vehicle combinations," Chalmers University of Technology, Tech. Rep., 2013.

[4] "European accident research and safety report 2013," Volvo Trucks, Tech. Rep., 2013.

[5] "Intelligent transport systems – lane change decision aid systems (lcdas) – performance requirements and test procedures," ISO 17387, 2008.

[6] http://www.teslamotors.com/blog/dual-motor-model-s-and-autopilot, 2015.02.21.

[7] J. Frasch, A. Gray, M. Zanon, H. Ferreau, S. Sager, F. Borrelli, and M. Diehl, "An auto-generated nonlinear mpc algorithm for real-time obstacle avoidance of ground vehicles," in *Control Conference (ECC), 2013 European*, 2013, pp. 4136–4141.

[8] S. M. LaValle and J. J. Kuffner, "Randomized kinodynamic planning," *The International Journal of Robotics Research*, vol. 20, no. 5, pp. 378–400, 2001.

[9] P. Nilsson, "Single-track models of an A-double heavy vehicle combination," Chalmers University of Technology, Tech. Rep. 8, 2013.

[10] P. Nilsson, L. Laine, O. Benderius, and B. Jacobson, "A driver model using optic information for longitudinal and lateral control of a long vehicle combination," in *Intelligent Transportation Systems (ITSC), 2014 IEEE 17th International Conference on*, 2014, pp. 1456–1461.

[11] D. D. Salvucci and R. Gray, "A two-point visual control model of steering," *Perception*, vol. 33, pp. 1233–1248, 2004.

[12] D. Lee, "A theory of visual control of braking based on information about time to collision," *Perception*, vol. 5, no. 4, pp. 437–459, 1976.

[13] H. B. Pacejka, *Tire and vehicle dynamics*. Butterworth-Heinemann, 2006.

[14] J. Albus and et.al., "4d/rcs a reference model architecture for intelligent unmanned ground vehicles," in *16th Annual International Symposium on Aerospace/Defense Sensing, Simulation and Controls (SPIE)*, 2002, pp. 1–8.

[15] J. Schröder, D. Holzner, C. Berger, C.-J. Hoel, L. Laine, and A. Magnusson, "Design and evaluation of a customizable multi-domain reference architecture on top of product lines of self-driving heavy vehicles - an industrial case study," in *37th International Conference on Software Engineering (ICSE 2015)*, 2015.

[16] L. Laine, "Reconfigurable motion control systems for over-actuated road vehicles," Ph.D. dissertation, Chalmers University of Technology, 2007.

[17] K. Tagesson, P. Sundstrom, L. Laine, and N. Dela, "Real-time performance of control allocation for actuator coordination in heavy vehicles," in *Intelligent Vehicles Symposium, 2009 IEEE*, 2009, pp. 685–690.

[18] K. Uhlen, P. Nyman, J. Eklöv, L. Laine, M. Sadeghi Kati, and J. Fredriksson, "Coordination of actuators for an a-double heavy vehicle combination using control allocation," in *Intelligent Transportation Systems (ITSC), 2014 IEEE*, 2014, pp. 641–648.